MEASUREMENT OF LOCAL HEAT TRANSFER COEFFICIENTS FOR FLOW OF HYDROGEN AND HELIUM IN A SMOOTH TUBE AT HIGH SURFACE TO FLUID BULK TEMPERATURE RATIOS

By Walter F. Weiland

E-1721

ABSTRACT

Local values of heat transfer coefficients have been measured experimentally for helium and hydrogen gas flowing through an electrically heated inconel tube. The experiment was conducted primarily to determine the effect on the heat transfer coefficient of a large density change, radially, in the heat transfer fluid.

This large density change was accomplished with relatively high surface temperatures as compared to fluid bulk temperatures or more commonly referred to as high surface to fluid bulk temperature ratio. The large temperature ratio was achieved by precooling the gas with liquid nitrogen.

Data were measured for local values of surface to fluid bulk temperature ratios up to 4.5, Reynolds numbers in the turbulent flow region, surface temperatures up to 2300° R, heat flux up to 1,600,000 Btu/(hr)(sq ft) and length to diameter ratio of 250.

A comparison of this data with the conventional heat transfer correlation equation (Dittus-Boelter eq.) is shown on a curve of Nusselt number divided by Prandtl number versus the Reynolds number. The gas properties were evaluated at the film temperature and the Reynolds number was modified by evaluating the velocity term at the fluid bulk temperature and the density at the film temperature.

Prepared for A.I.Ch.E.
Symposium on Nuclear
Engineering Heat Transfer
Chicago, Illinois, Dec. 1962

E-1721

MEASUREMENT OF LOCAL HEAT TRANSFER COEFFICIENTS FOR FLOW OF HYDROGEN AND HELIUM IN A SMOOTH TUBE AT HIGH SURFACE TO FLUID BULK TEMPERATURE RATIOS

By Walter F. Weiland

Lewis Research Center
National Aeronautics and Space Administration
Cleveland, Ohio

INTRODUCTION

The interest in convective heat transfer with large variations in fluid properties has been stimulated by the importance of nuclear reactors as a source of power for space vehicles. Here the ratio of fuel element-to-working fluid temperature, and hence the variation of fluid properties, can be quite large near the inlet of a nuclear reactor if the fluid enters at near cryogenic temperature.

Experimental data showing the effect of the variation of surface-to-fluid bulk temperature ratio on the heat transfer coefficient for gases are contained in reference 1. Average heat transfer coefficients were correlated using the Dittus-Boelter equation and evaluating the fluid properties, including the density term in the Reynolds number, at the film temperature. The film temperature is the arithmetic average of the bulk and surface temperature. The range of conditions covered in the investigation (ref. 1) were as follows: T_s/T_b up to 3.5, L/D of 30 to 120, average surface temperature up to 3050° R. These conditions were extended (ref. 2) to

T_s/T_b of 3.9 for a L/D of 60 to 91. Some local values of heat transfer coefficient have been measured (ref. 3) for T_s/T_b up to 11.09 and for L/D of 20.9 to 42.6.

The equation used for correlation of heat transfer coefficients in reference 1 predicts a minimum value in the wall temperature profile for large T_s/T_b, constant heat flux and a large length-to-diameter ratio, L/D. Since in the previous investigations the data obtained for constant heat flux and large T_s/T_b ~~was~~ were for tubes of short L/D, an investigation was conducted at NASA Lewis Research Center for the following conditions: Length-to-diameter ratio of 250, surface-to-gas bulk temperature ratio up to 4 and Reynolds number from 30,000 upward. Data ~~was~~ were obtained for both hydrogen and helium gas flowing through a smooth tube with constant heat flux.

EXPERIMENTAL APPARATUS

Apparatus

A schematic diagram of the piping and associated equipment is shown in figure 1. Either hydrogen or helium gas was used as the heat transfer fluid. The supply gas pressure is first reduced to 1500 psi by a pressure reducing valve. The gas pressure desired for the test is then set with a remotely operated pressure regulating valve. The gas flow is metered with a sharp edge orifice located downstream of the pressure regulating valve. From the orifice the gas passes through a coil placed in a thermally insulated tank. This tank is filled with liquid nitrogen when low inlet gas temperatures are desired. After the coils the gas flows through

the inlet mixing tank, the test section and the outlet mixing tank. The gas is then cooled in a water-to-gas heat exchanger before it passes through a flow control valve and is exhausted to the atmosphere.

The test section and mixing tanks were enclosed in a pressure vessel filled with helium gas at a pressure slightly greater than at the inlet to the test section. This was done to avoid excessive stresses on the test section at high temperatures. The system used for pressurizing the vessel is independent of the flow system.

Test Section and Mixing Tanks

A drawing of the test section and mixing tanks is shown in figure 2. The test section was fabricated from commercial inconel tubing having a O.D. of 0.250 inch, a wall thickness of 0.031 inch, a heated length of 48 inches and a length-to-diameter ratio of 255. The unheated straight tube approach to the test section had a length-to-diameter ratio of 10.6.

The test section was thermally insulated by one of two methods. The first method consisted of radiation shields surrounding the test section and zirconia bubbles packed between the shields and the wall of the pressure vessel. Since there was an abnormally large amount of thermocouple breakage a second method of insulating was used so that the length of unsupported thermocouple lead wire could be reduced. This method employed a 4-inch diameter aluminum cylinder surrounding the test section. The cylinder was packed with magnesia

and pyrex wool. This proved to be satisfactory and no more than normal thermocouple breakage occurred.

Helium data was obtained using the first method of insulating the test section and hydrogen data was obtained using the second method.

Instrumentation

The outside wall temperatures of the test section were measured with copper-constantan and Chromel-Alumel thermocouples. The Chromel-Alumel thermocouples were spot welded to the test section. Except for short sections near the inlet and outlet of the test section, the thermocouples were evenly spaced at 2 or 4 inch intervals along the test section depending on the number of lead wires available. Since the wall temperature changes rapidly near the inlet and outlet of the test section, the thermocouples were spaced closer together in these regions to obtain reliable wall temperature profiles.

Three copper-constantan thermocouples were brazed to the test section at approximately 1/4, 3/4, and $1\frac{1}{2}$ inches from the inlet. These were used to measure the wall temperatures that were well below ambient as was the case for some tests when the gas was precooled.

A copper-constantan thermocouple was used to measure the gas temperature at the inlet to the test section and a Chromel-Alumel thermocouple was used to measure the outlet gas temperature. These thermocouples were located downstream of the screens in the mixing

tanks. Static pressure taps were located at the inlet and outlet of the test section as shown in figure 2.

A sharp edge orifice calibrated for use with helium or hydrogen was used to measure the gas flow. The pressure drop across the orifice was measured with a high pressure glass manometer using mercury as the fluid.

METHOD OF CALCULATIONS

Gas Properties

The physical properties of helium used in calculating the Nusselt and Reynolds numbers were obtained from references 2 and 4, and are shown in figure 3 as a function of temperature. The specific heat is 1.24 Btu/(lb)(^{o}R) and is constant.

The physical properties of hydrogen at pressures of 1 and 100 atmospheres are shown in figure 4(a), (b), and (c) as a function of temperature. Values of thermal conductivity and viscosity were obtained from references 5 and 6. The specific heat was obtained from references 5 and 7.

Heat Transfer Coefficients

Heat transfer coefficients were calculated for small increments of the test section. Although these heat transfer coefficients represented average values, by choosing small increments the variation in heat flux over an increment was negligible and the temperature rise of the gas and tube wall was small so that the calculated values very nearly represented the local heat transfer coefficients at the midpoint of the increment. The incremental

method of calculation was used since a heat balance can readily be determined for each increment along the tube and the bulk temperature of the gas can then be calculated from the resulting temperature rise of the gas for each increment.

Identification of some of the symbols, at this time, will be of value in following the calculation procedure. The inlet of the increment is identified by the superscript (') and the outlet by (''). The subscript (n) refers to the n^{th} increment. The heat transfer coefficient was calculated from the equation:

$$h = \frac{Q}{S(T_{s,n} - T_{b,n})} \tag{1}$$

The heat transferred to the gas Q is expressed by the heat balance equation

$$Q = Q_g + Q_c - Q_L \tag{2}$$

Here Q_g is the heat generated in an increment corrected to give a heat balance of 100 percent by the equation:

$$Q_g = \left[\frac{Wc_p(T_{ex} - T_{in})}{\sum Q_e + \sum Q_c - \sum Q_i} \right] Q_e \tag{3}$$

This correction was generally only a few percent.

Q_c in equation (2) is the net heat conducted axially into the increment and Q_L is the heat lost to the surroundings. The heat lost to the surroundings was measured at various temperatures and pressures by applying power to the test section with no gas flow and allowing the equipment to reach thermal equilibrium. The heat

being generated was then considered to be equal to the heat loss to the surroundings at that particular pressure and average outside wall temperature.

The gas temperature $T_{b,n}$ is the arithmetic average gas temperature between the inlet and outlet of the increment.

The inside wall temperature $T_{s,n}$ was taken as the average outside wall temperature integrated along the lenth of the increment $T_{w,n}$ minus the temperature drop through the wall and was calculated from the following equation derived in reference 8 and modified to include the heat loss to the surroundings

$$T_{s,n} = T_{w,n} - \left[\frac{Q_g}{(r_o^2 - r_i^2)(2k_n\pi\,\Delta X)}\right]\left[r_o^2 \ln\frac{r_o}{r_i} - \left(\frac{r_o^2 - r_i^2}{2}\right)\right] + \frac{Q_L \ln\frac{r_o}{r_i}}{2k_n\pi\,\Delta X} \qquad (4)$$

The equation assumes the heat is produced in the tube uniformly across the tube wall thickness.

The average bulk gas temperature $T_{b,n}$ is calculated from the equation:

$$T_{b,n} = \frac{T_n'' + T_n'}{2} \qquad (5)$$

where

$$T_n'' = T_{n+1}' = T_n' + \frac{Q}{Wc_p} \qquad (6)$$

Since T_n' must be known to solve the equations (5) and (6), the

calculations were started with the first increment where T_1^i is equal to the measured temperature T_{in} and calculation must proceed in order toward the exit.

RESULTS AND DISCUSSION

Axial Wall Temperature Distribution

The axial wall temperature distribution is a straight line variation if the heat transfer coefficient and heat flux are constant with X/D. The heat transfer coefficient is constant with X/D for fully developed flow and constant fluid properties. However, with variable fluid properties the heat transfer coefficient is no longer constant with X/D and then for constant heat flux this variation of the heat transfer coefficient is reflected in the axial wall temperature distribution. This can be seen in figure 5 where the measured outside wall temperature is plotted as a function of X/D for various average heat fluxes for the test section. The maximum variation of heat flux over the entire length of the test section was 4 percent. Runs number 108 and 107 show the effect of a large axial variation of fluid properties (large axial variation of T_s/T_b) on the wall temperature distribution. At high T_s/T_b values and large enough X/D where the wall temperature was not influenced by end effects, the wall temperature actually decreased with increasing X/D. A curve of the same general shape is predicted by the Dittus-Boelter equation when the properties, including the density term in the Reynolds number, are evaluated at the same temperature. Included for comparison are runs 85 and 72. Here the

axial variation of fluid properties is relatively small (small axial variation of T_s/T_b). These runs show a nearly straight line variation of the axial wall temperature distribution.

Gas flow, inlet and outlet gas temperature, heat flux and T_s/T_b at various X/D are tabulated on the figure. These data are for hydrogen gas, however, similar axial wall temperature distributions were obtained for helium gas.

Correlation of Local Heat Transfer Coefficient

The results presented in reference 1 for turbulent flow in tubes indicates that the average Nusselt number decreases progressively as the ratio of surface-to-bulk temperature increases. A correlation was obtained by evaluating the fluid properties, including the density term in the Reynolds number at either the surface or film temperature.

This method of correlating the average heat transfer coefficients was applied to the local heat transfer coefficients obtained in this investigation and is shown in figures 6(a) and (b) for hydrogen gas and figures 6(c) and (d) for helium gas. The Nusselt number is plotted as a function of the Reynolds number at X/D values of 72, 130, and 226. Included for comparison is the line represented by the equation:

$$\frac{hD}{K_a} = 0.021 \left(\frac{\rho_a V_b D}{\mu_a}\right)^{0.8} \left(\frac{c_p \mu}{K}\right)_a^{0.4} \qquad (7)$$

where the subscript, a, refers to the reference temperature at which the properties are evaluated. The data using either surface

or film correlation are in fair agreement with the predicted line.

Inasmuch as equation (7) includes the effect of variable properties (T_s/T_b) one would expect that for fully developed temperature and velocity profiles ($X/D > 15$) the relation between Nusselt, Reynolds, and Prandtl numbers is fixed and independent of X/D.

Figures 7(a) and (b) show the variation of the relation between Nusselt, Reynolds, and Prandtl numbers with X/D for both small axial variations of T_s/T_b (run 85) and large axial variations in T_s/T_b (run 108). The axial wall temperature distributions for these data is shown in figure 5. Large values of T_s/T_b (run 108) were obtained by cooling the gas with liquid nitrogen before it entered the test section. These two runs are representative of the data for helium and hydrogen gas inasmuch as they show the general trend of the data.

Examination of the two figures indicate that for the case of small axial variations of fluid properties the Nusselt-Reynolds relation is nearly independent of X/D, after a small X/D, when the fluid properties are evaluated at the film temperature. However, for large axial variation in fluid properties the Nusselt-Reynolds number relation varies with X/D when the fluid properties are evaluated at either the film or surface temperature.

The fact that the relation between the Nusselt, Reynolds, and Prandtl is not independent of X/D leads to the conclusion that the temperature profile is not fully developed. This conclusion

seems reasonable in that with variable properties the temperature profile is continually changing.

A correlation of the data was not undertaken at this time as it was felt more data must be obtained to investigate high T_s/T_b with small axial variations and data similar to that obtained in this investigation but at higher surface-to-bulk temperature ratios.

SYMBOLS

c_p	specific heat of gas at constant pressure, Btu/(lb)(^oR)
D	inside diameter of test section, ft
h	heat transfer coefficient, Btu/(sec)(sq ft)(^oR)
K	thermal conductivity of gas, Btu/(sec)(sq ft)(^oR/ft)
k	thermal conductivity of test section material, Btu/(sec)(sq ft)(^oR/ft)
L	length of test section (heated section), ft
Q	heat transferred to the gas per increment, Btu/sec
Q_c	net heat transferred axially into increment, Btu/sec
Q_e	heat generated electrically in an increment, Btu/sec
Q_g	corrected heat generated per increment, Btu/sec
Q_L	heat loss radially to surroundings per increment, Btu/sec
r_i	inside radius of test section, ft
r_o	outside radius of test section, ft
S	inside surface area of increment, sq ft
T	bulk temperature of gas, ^oR
T_b	average bulk gas temperature of increment, ^oR
T_{ex}	measured gas temperature at exit of test section, ^oR
T_f	film temperature of gas, $T_s + T_b/2$, ^oR
T_{in}	measured gas temperature at inlet of test section, ^oR
T_s	average inside wall temperature of increment, ^oR
T_w	average outside wall temperature of increment, ^oR
V	velocity, ft/sec
W	gas flow, lb/sec

X distance from inlet of test section (heated section), ft

ΔX length of increment, ft

μ absolute viscosity of gas, lb/sec-ft

ρ density of gas, lb/(cu ft)

Subscripts

b bulk (when applied to properties, indicates evaluation at bulk temperature, T_b)

f film (when applied to properties, indicates evaluation at film temperature, T_f)

n any segment

s surface (when applied to properties, indicates evaluation at surface temperature, T_s)

Superscripts

' inlet of increment

" outlet of increment

LITERATURE CITED

1. Humble, L. V., Lowdermilk, W. H., and Desmon, L. G., "Measurements of Average Heat-Transfer and Friction Coefficients for Subsonic Flow of Air in Smooth Tubes at High Surface and Fluid Temperatures," NACA Rep. 1020 (1951).

2. Taylor, M. F., and Kirchgessner, T. A., "Measurements of Heat Transfer and Friction Coefficients for Helium Flowing in a Tube at Surface Temperatures up to 5900° R," NASA TN D-133 (1959).

3. Wolf, H., and McCarthy, J.R., "Heat Transfer to Hydrogen and Helium with Wall to Fluid Temperature Ratios to 11.09," Rocketdyne Division, North American Aviation, Inc., Canoga Park, California. Presented at A.I.Ch.E. Annual Meeting, Washington, D. C. (December, 1960).

4. "Hydrogen Handbook," Arthur D. Little, Inc., Parker Aircraft Co., Air Force Flight Test Center (1960). Contract AF-33(610)-6710.

5. King, C. R., "Compilation of Thermodynamic Properties, Transport Properties, and Theoretical Rocket Performance of Gaseous Hydrogen," NASA TN D-275 (1960).

6. Svehla, R. A., "Estimated Viscosities and Thermal Conductivities of Gases at High Temperatures," NASA TR R-132 (1962).

7. Hilsenrath, Joseph, et al., "Tables of Thermal Properties of Gases," Cir. 564, NBS (November 1, 1955).

8. Bernardo, E., and Eian, C. S., "Heat-Transfer Tests of Aqueous Ethylene Glycol Solutions in an Electrically Heated Tube," NACA ARR E5F07, 1945.

FIGURE LEGENDS

Fig. 1. - Schematic of piping and associated equipment.

Fig. 2. - Test section and mixing tank assembly.

Fig. 3. - Variation of thermal conductivity and viscosity of helium with temperature.

(a) Variation of thermal conductivity with temperature.

(b) Variation of viscosity with temperature.

(c) Variation of specific heat with temperature.

Fig. 4. - Physical properties of hydrogen at 1 and 100 atmospheres.

Fig. 5. - Representative wall temperature distribution.

(a) Fluid properties evaluated at film temperature, hydrogen gas.

(b) Fluid properties evaluated at surface temperature, hydrogen gas.

(c) Fluid properties evaluated at film temperature, helium gas.

(d) Fluid properties evaluated at surface temperature, helium gas.

Fig. 6. - Correlation of local heat transfer coefficient.

(a) Fluid properties evaluated at film temperature.

(b) Fluid properties evaluated at surface temperature.

Fig. 7. - Variation of Nusselt-Reynolds number relation with distance from inlet for hydrogen gas.

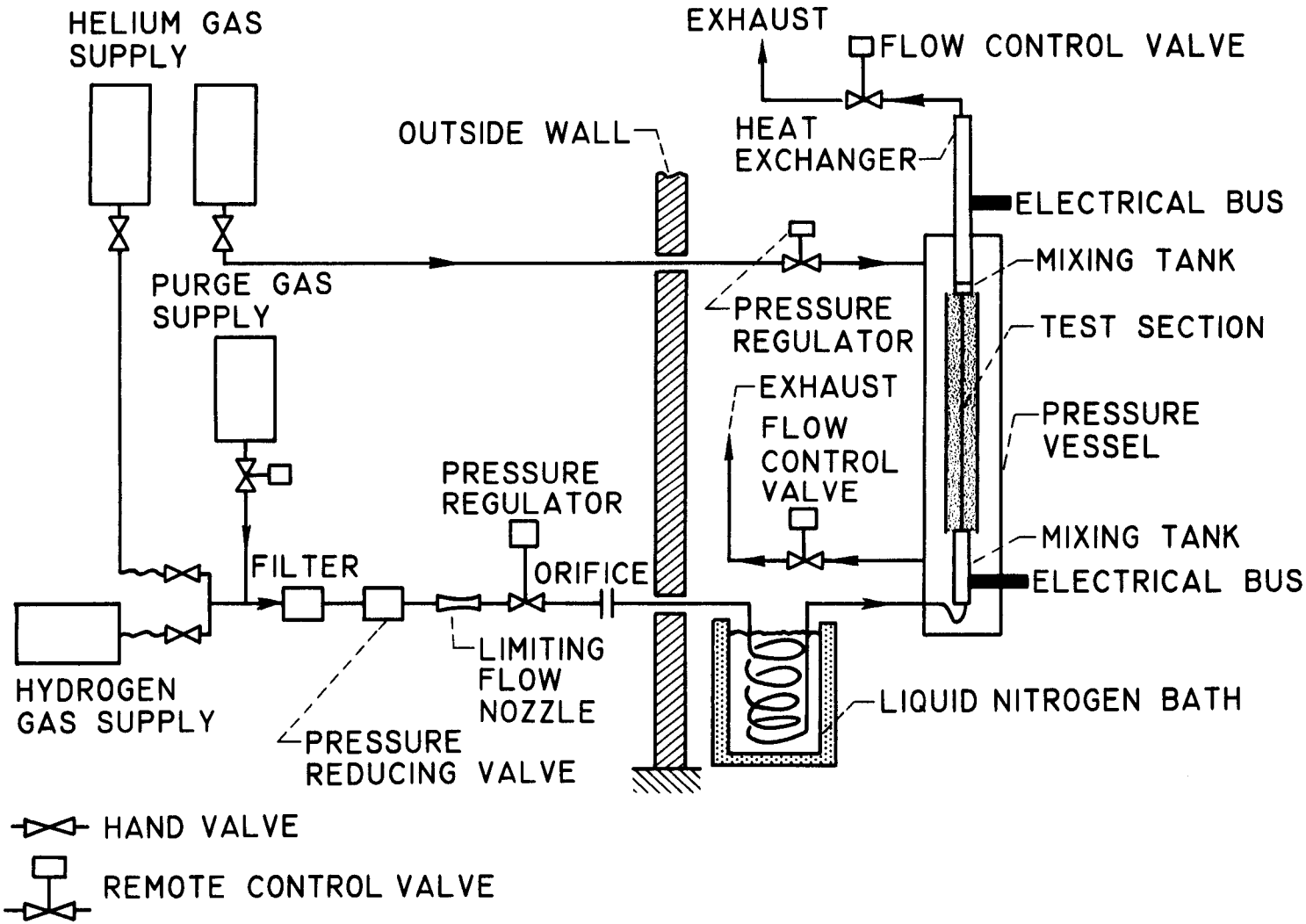

Fig. 1. - Schematic of piping and associated equipment.

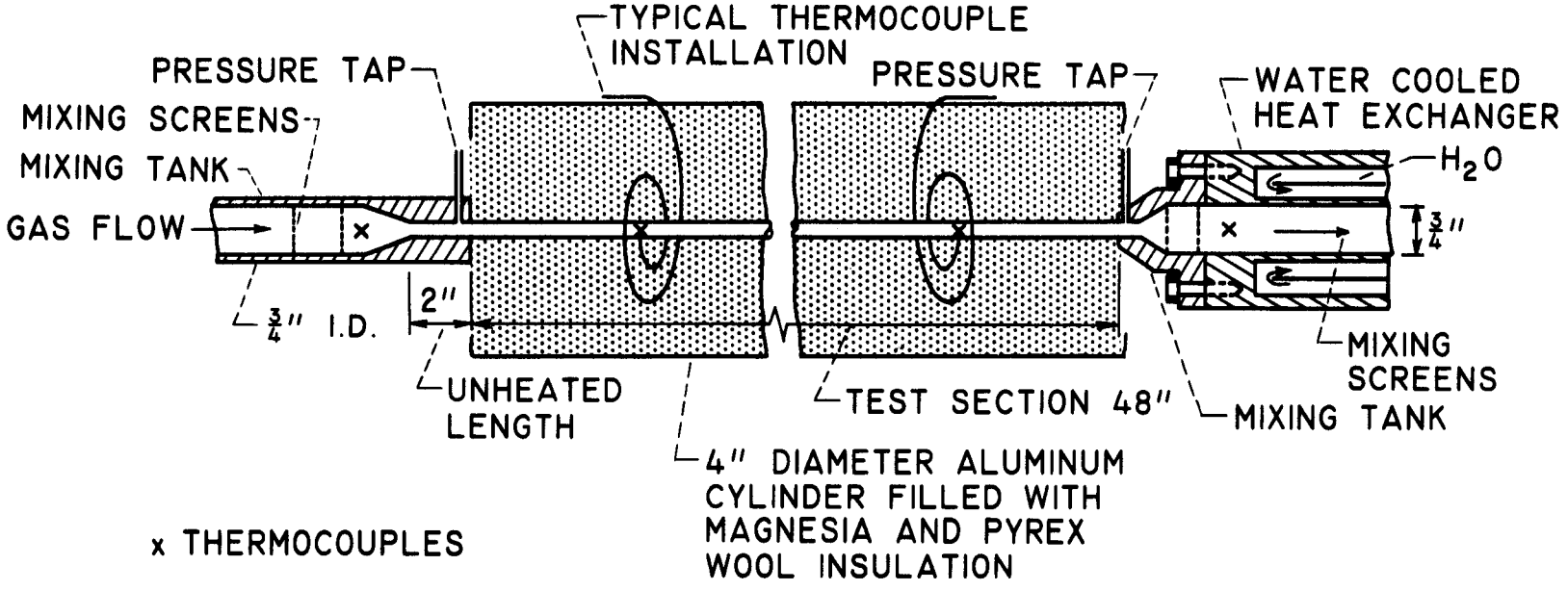

Fig. 2. - Test section and mixing tank assembly.

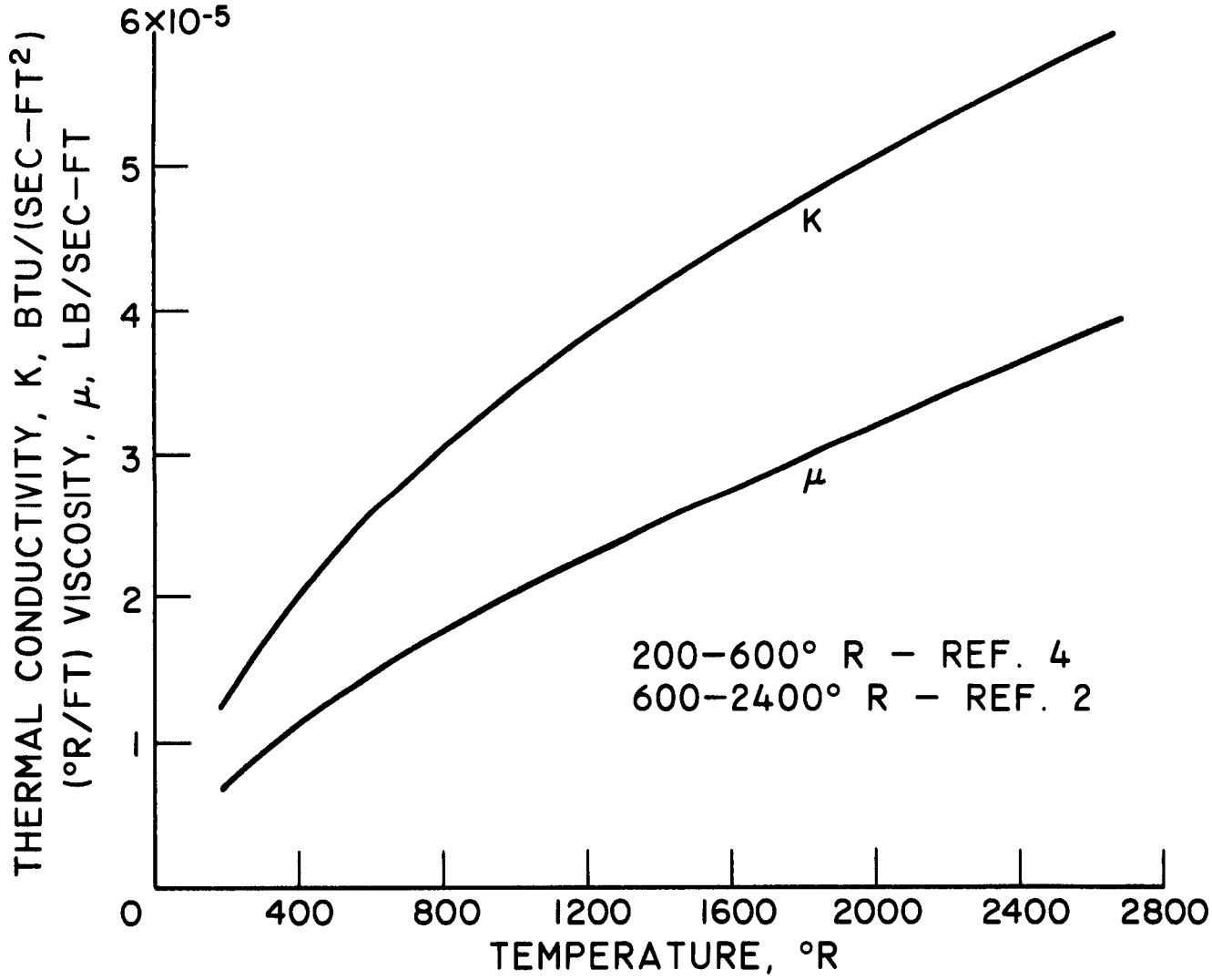

Fig. 3. - Variation of thermal conductivity and viscosity of helium with temperature.

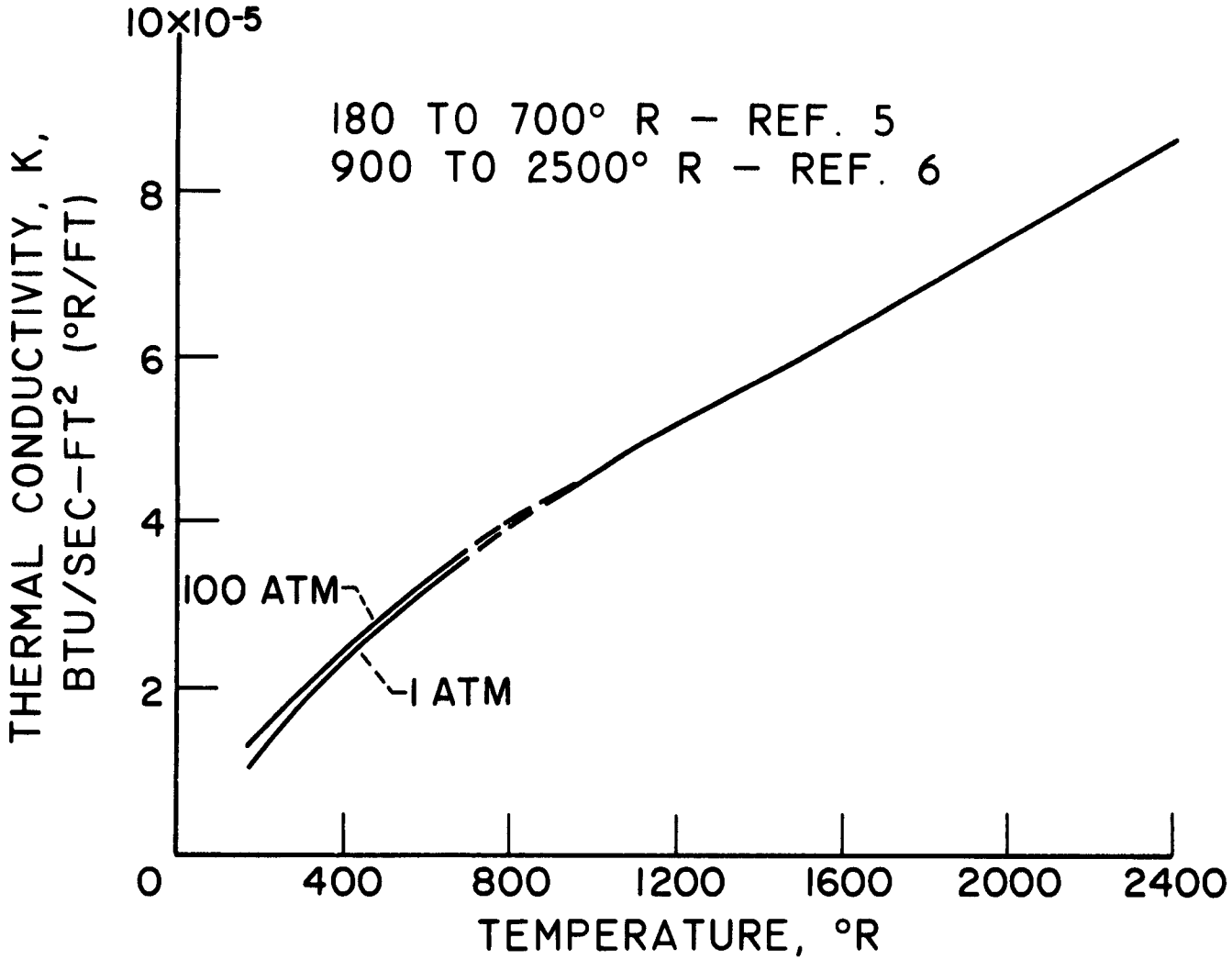

Fig. 4a. - Physical properties of hydrogen at 1 and 100 atmospheres, variation of thermal conductivity with temperature.

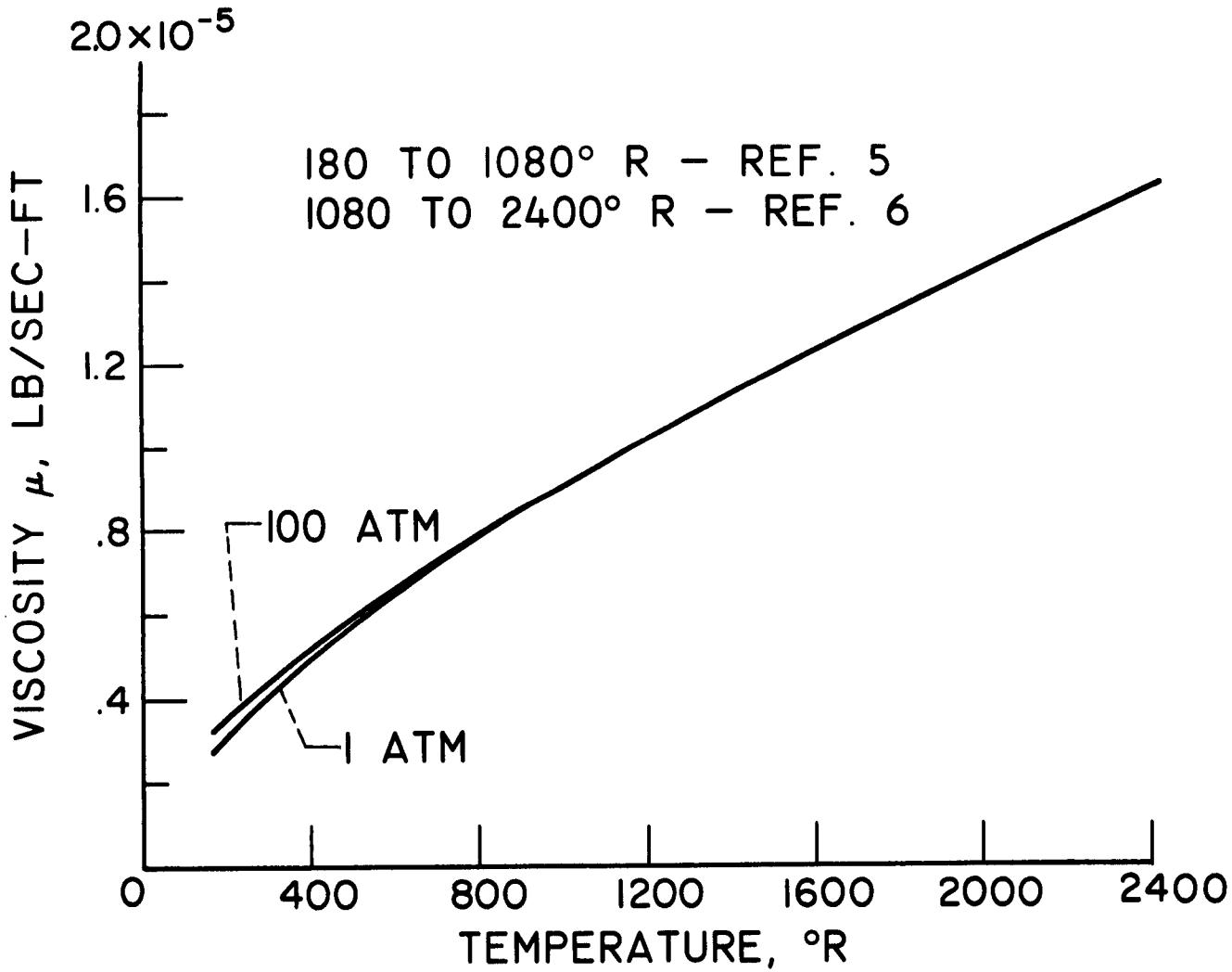

Fig. 4b. - Physical properties of hydrogen at 1 and 100 atmospheres, variation of viscosity with temperature.

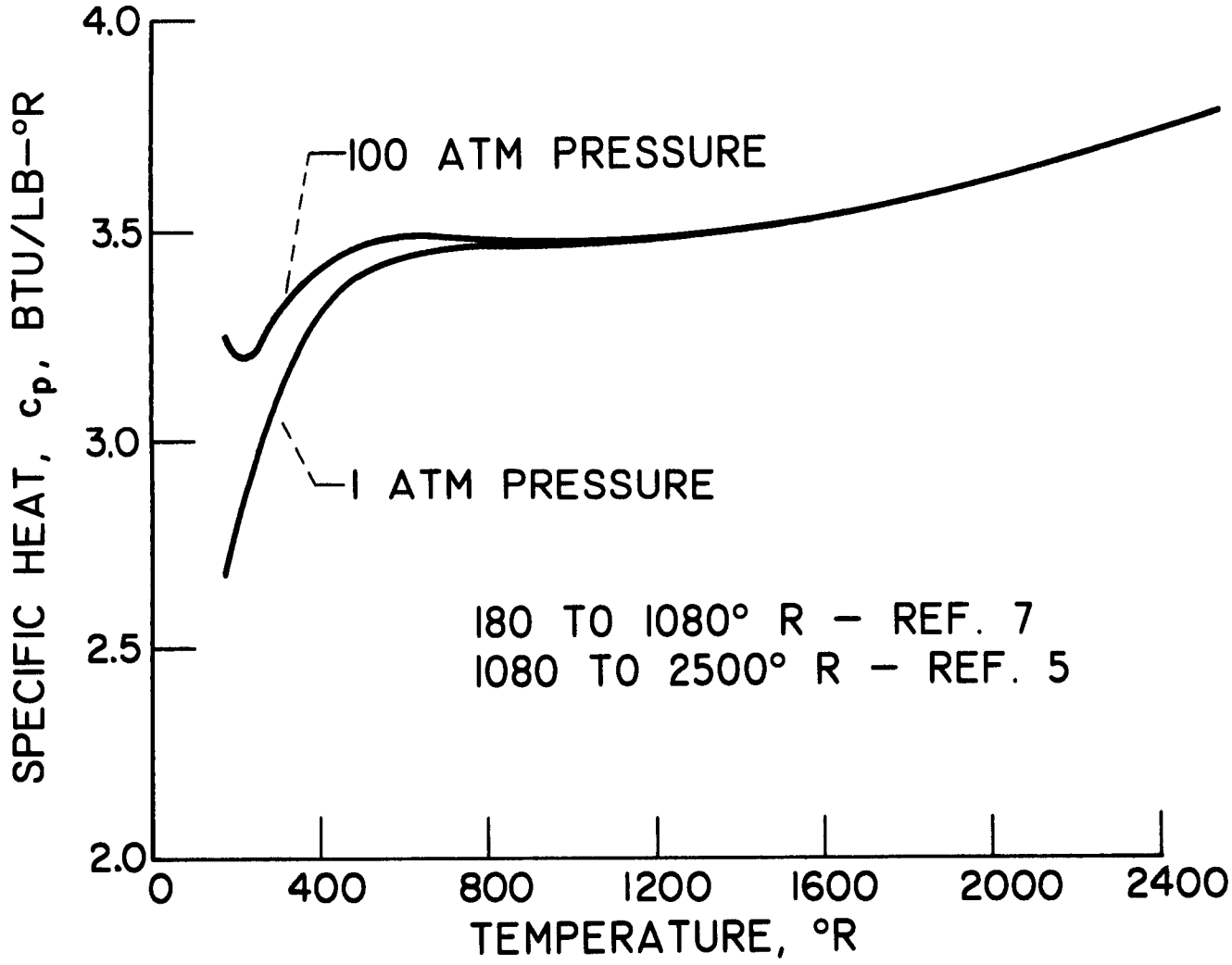

Fig. 4c. - Concluded. Physical properties of hydrogen at 1 and 100 atmospheres, variation of specific with temperature.

E-1721

	RUN NO.	W, LB/SEC	$(Q/S)_{ave.}$ BTU/SEC-FT^2	T_{in}, °R	T_{ex}, °R	T_s/T_b X/D		
						13.3	66	226
◇	85	.0130	272	548	1733	1.92	1.69	1.30
○	108	.0129	316	238	1638	4.43	2.80	1.39
□	72	.0132	182	536	1318	1.60	1.50	1.26
△	107	.0129	229	222	1248	3.28	2.55	1.40

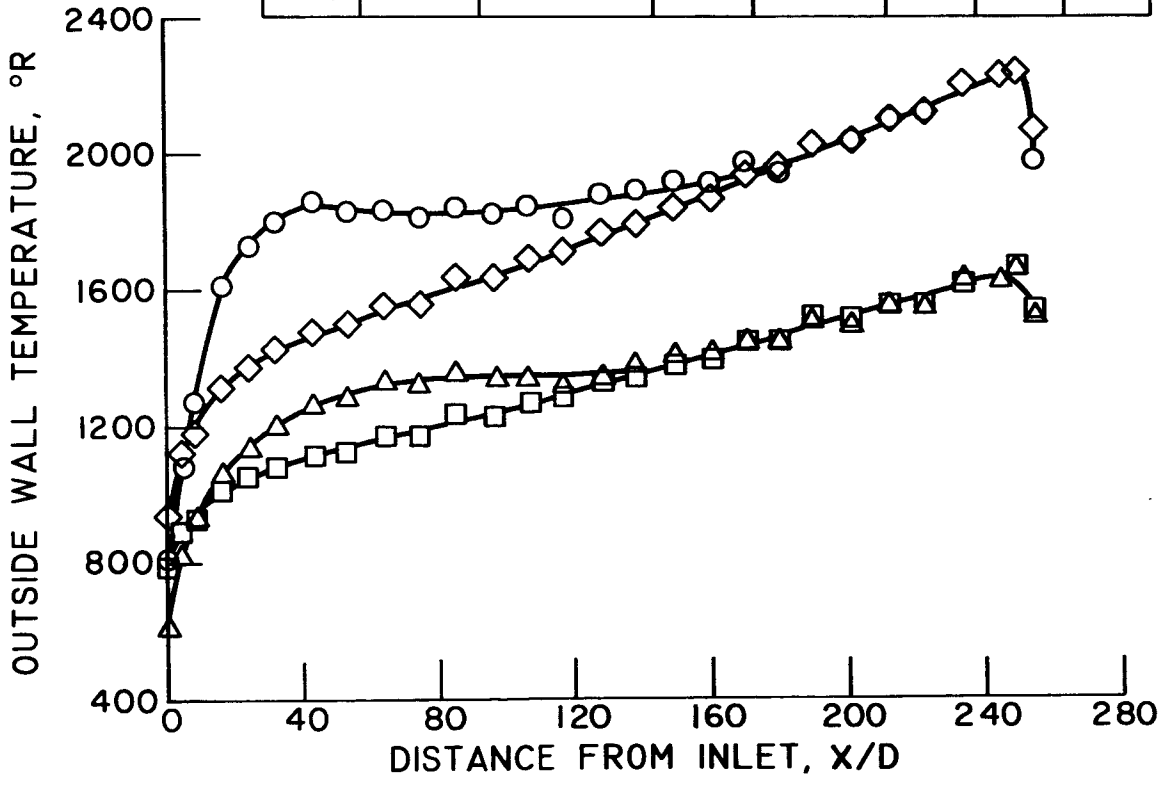

Fig. 5. - Representative wall temperature distribution.

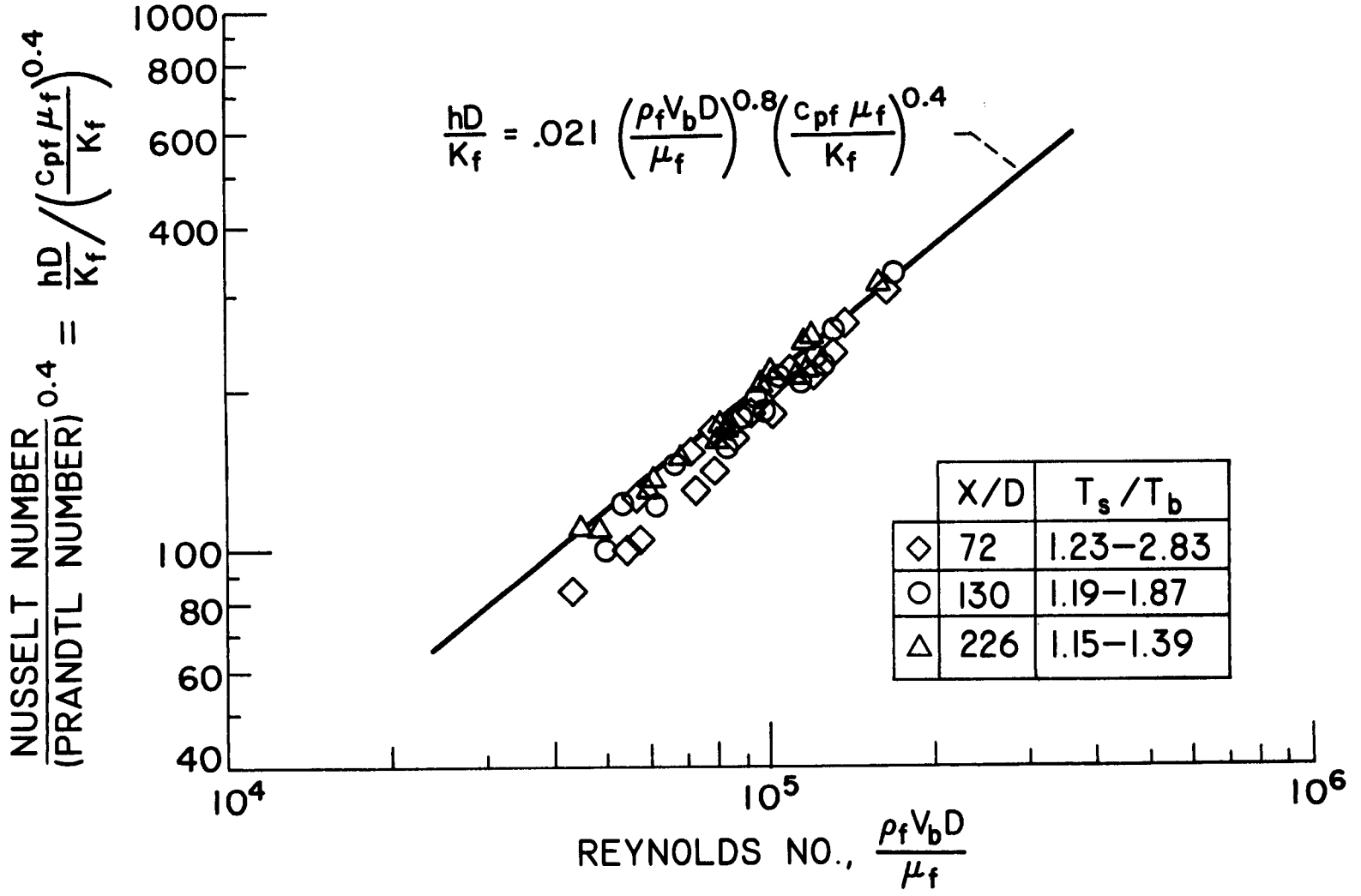

Fig. 6a. - Correlation of local heat transfer coefficient, fluid properties evaluated at film temperature, hydrogen gas.

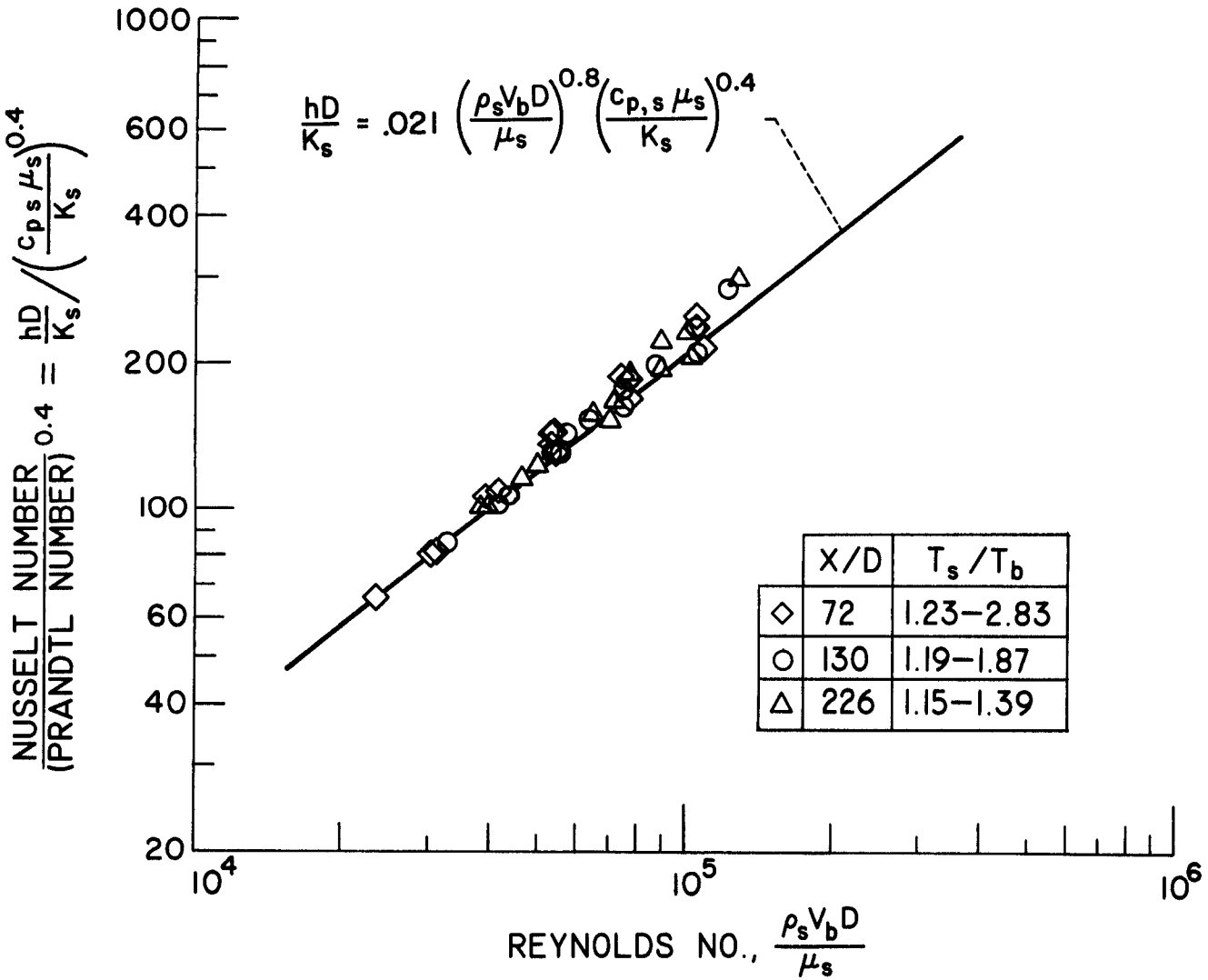

Fig. 6b. - Correlation of local heat transfer coefficient, fluid properties evaluated at surface temperature, hydrogen gas.

E-1721

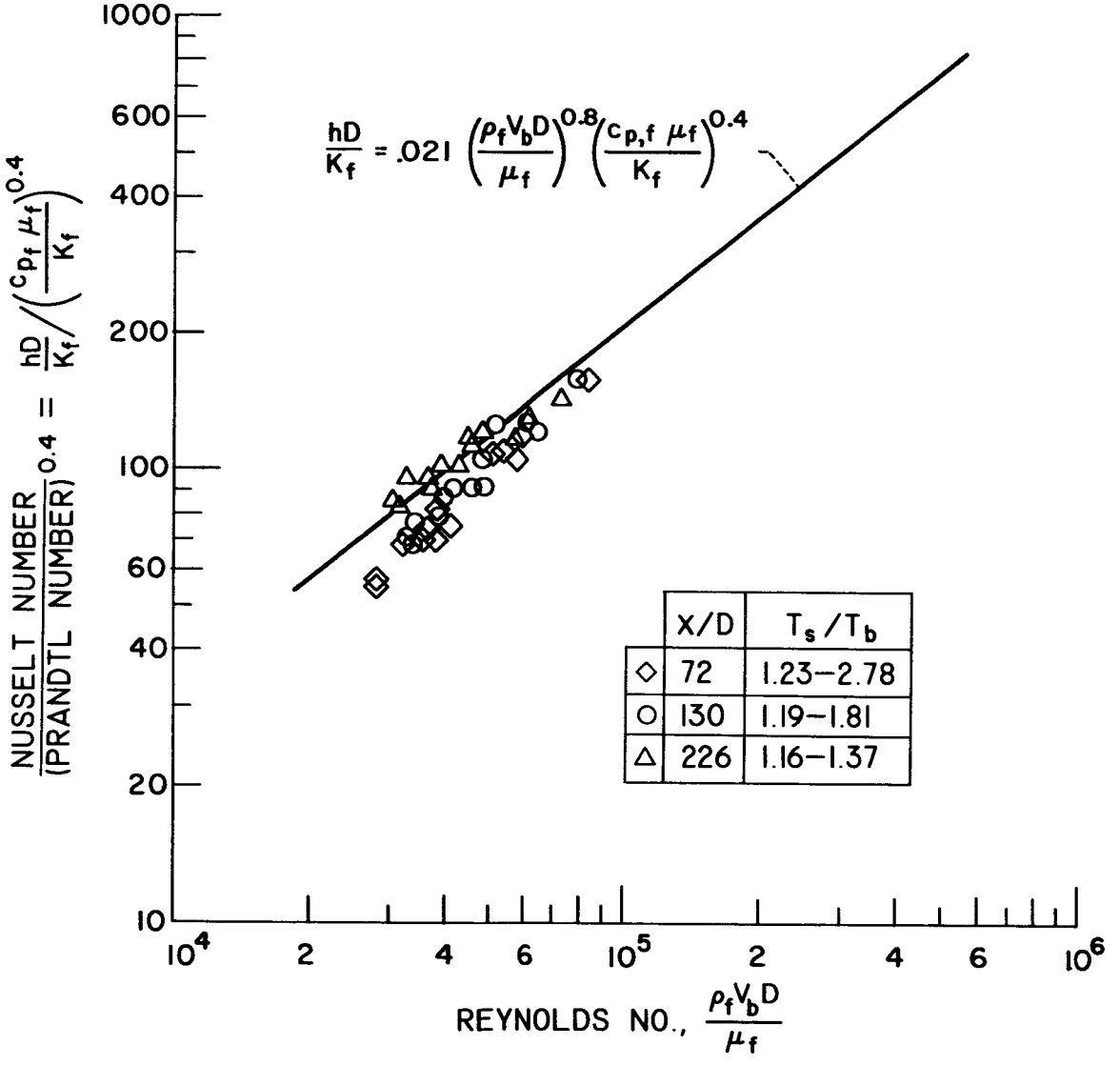

Fig. 6c. - Correlation of local heat transfer coefficient, fluid properties evaluated at film temperature, helium gas.

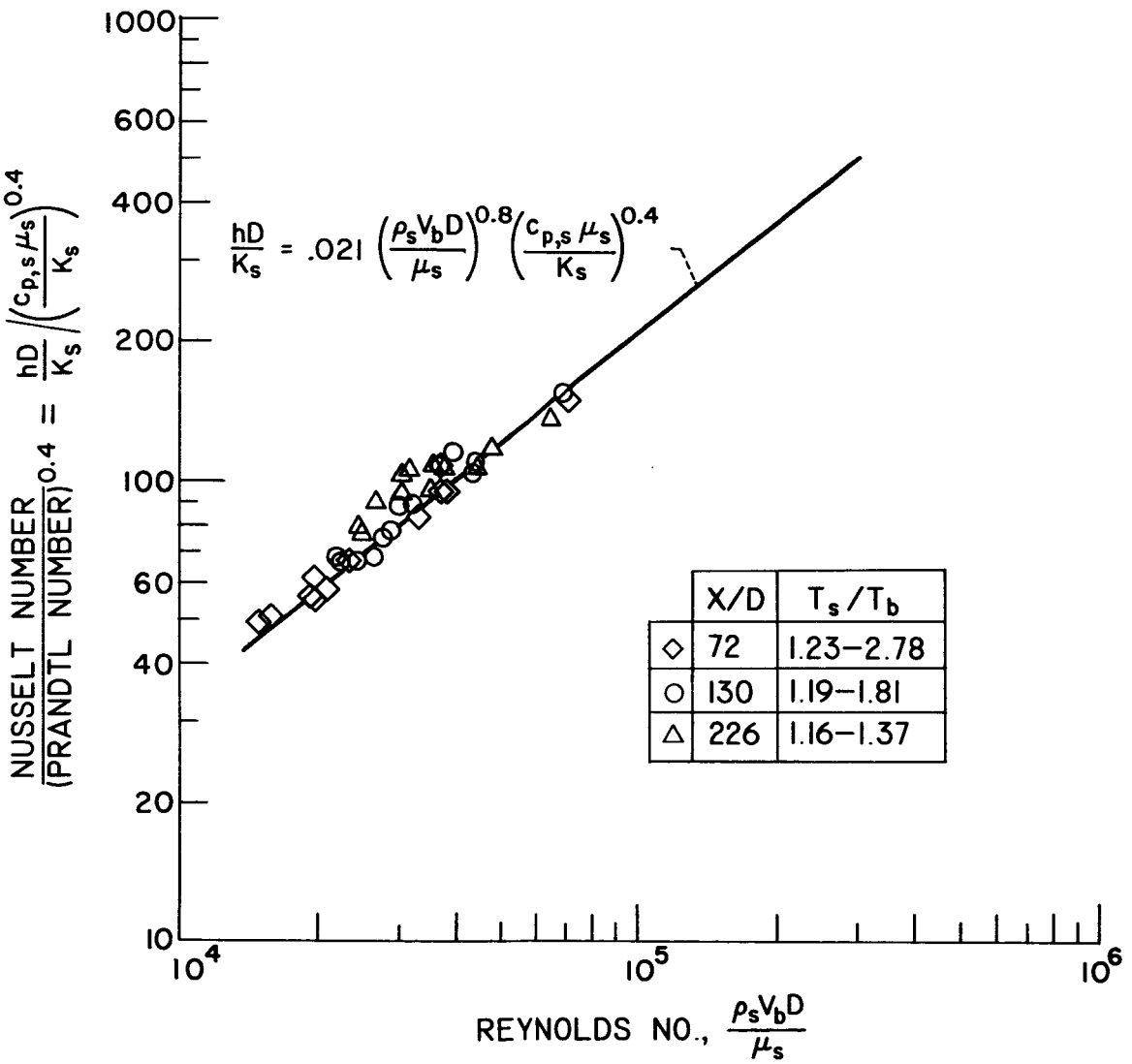

Fig. 6d. - Concluded. Correlation of local heat transfer coefficients, fluid properties evaluated at surface temperature, helium gas.

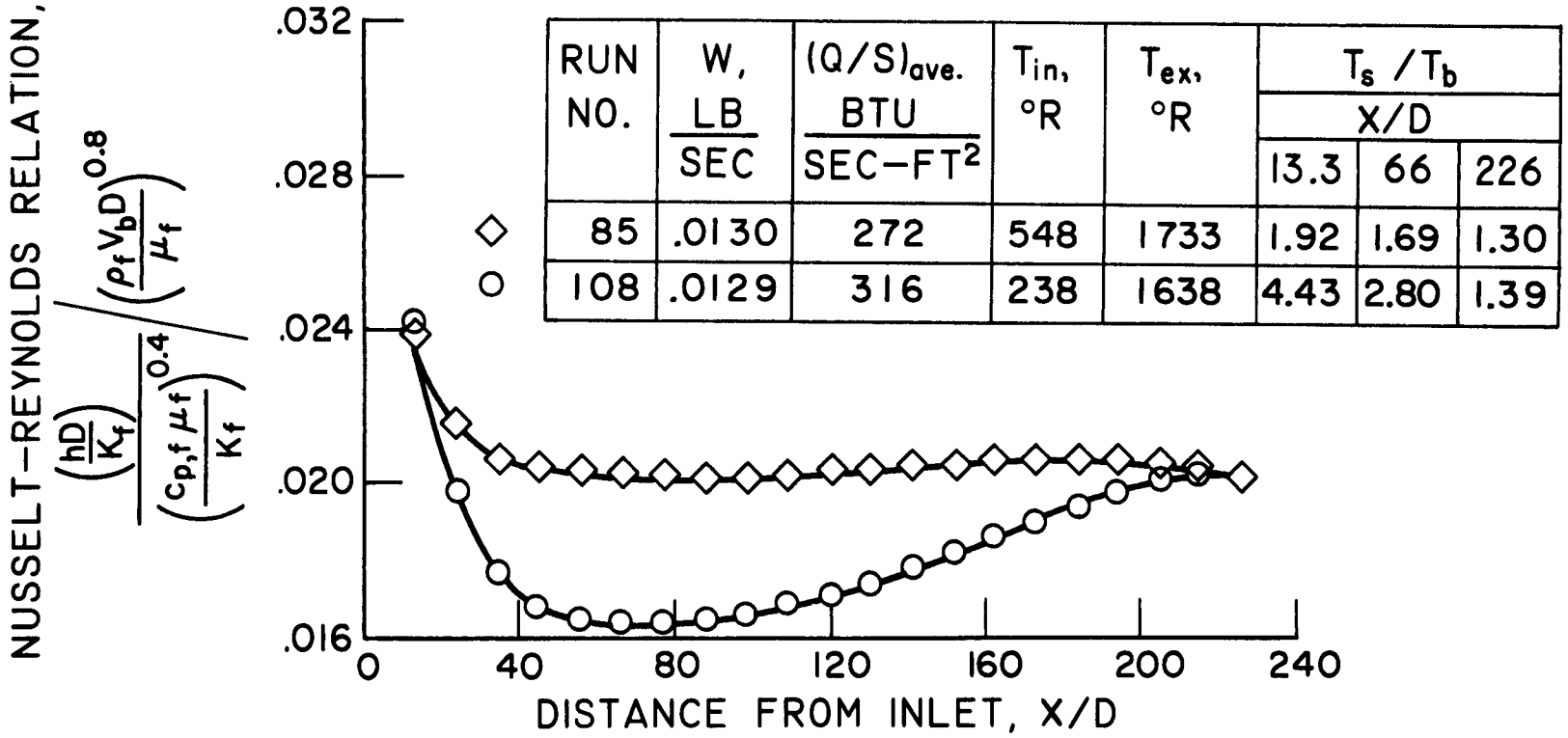

RUN NO.	W, LB/SEC	$(Q/S)_{ave.}$ BTU/SEC-FT^2	T_{in}, °R	T_{ex}, °R	T_s / T_b X/D		
					13.3	66	226
◇ 85	.0130	272	548	1733	1.92	1.69	1.30
○ 108	.0129	316	238	1638	4.43	2.80	1.39

Fig. 7a. - Variation of Nusselt-Reynolds number relation with distance from inlet for hydrogen gas, fluid properties evaluated at film temperature.

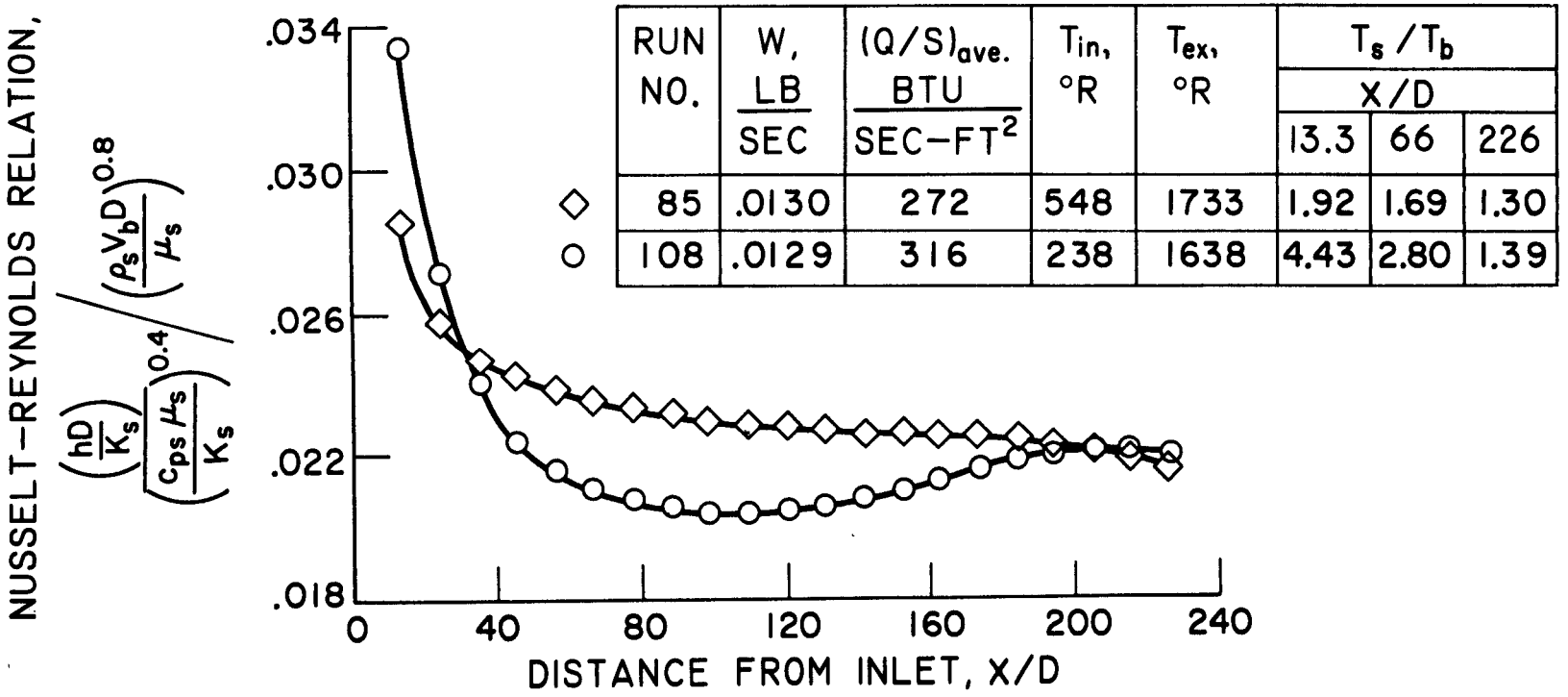

	RUN NO.	W, LB/SEC	$(Q/S)_{ave.}$ BTU/SEC-FT^2	T_{in}, °R	T_{ex}, °R	T_s/T_b X/D = 13.3	T_s/T_b X/D = 66	T_s/T_b X/D = 226
◇	85	.0130	272	548	1733	1.92	1.69	1.30
○	108	.0129	316	238	1638	4.43	2.80	1.39

Fig. 7b. - Concluded. Variation of Nusselt-Reynolds number relation with distance from inlet for hydrogen gas, fluid properties evaluated at surface temperature.

NASA-CLEVELAND, OHIO E-1721